RSC Advances

PAPER

View Article Online
View Journal | View Issue

Cite this: *RSC Adv.*, 2021, **11**, 4660

Preparation of fluorine-free superhydrophobic and wear-resistant cotton fabric with a UV curing reaction for self-cleaning and oil/water separation

Yaofa Luo,[a] Shuang Wang,[a] Xihan Fu,[a] Xiaosheng Du,[ab] Haibo Wang,[ab] Xu Cheng*[ab] and Zongliang Du*[ab]

A durable superhydrophobic, self-cleaning cotton fabric prepared with UV curing was prepared by a simple method and used for oil/water separation. Firstly, sulfhydryl silica nanoparticles on the fabric surface were prepared by the Stöber reaction (SiO_2–SH@cotton). Then, the side chain hydroxyl terminated PDMS was reacted with isocyanate to form an isocyanate terminated prepolymer. The prepolymer terminated by HEMA (vinyl-terminated PDMS (PIH)) was sprayed on the fabric surface, and then the superhydrophobic coating (SiO_2–S–PIH@cotton) was formed using UV curing. A series of characterization methods were used to demonstrate the properties of the modified cotton fabric. When the weight gain after PIH spraying was 1.8 wt%, the fabric reaches an optimal state (water contact angle (WCA) of 153° and a sliding angle of 7°). When used in an oil–water separation test, the highest separation efficiency reached 99.1%. In particular, the as-prepared fabric has excellent wear resistance. Compared with that before spraying, the superhydrophobicity of the as-prepared fabric has no obvious decrease after 300 cycles under 200 g of weight or after 100 cycles under 500 g of circular friction. This indicated that surface sprayed polymers have two functions: providing low surface tension and protecting the rough surface formed by silica particles. This process was time-saving, energy-saving, protected the environment, had a low material cost and a strong performance stability. It is hoped that this fabric can be used in the large-scale industrialization of oil–water separation.

Received 28th November 2020
Accepted 5th January 2021

DOI: 10.1039/d0ra10060a

rsc.li/rsc-advances

1. Introduction

Superhydrophobic surfaces have attracted wide interest because of their potential applications in self-cleaning, anti-corrosion, anti-icing, oil–water separation, and so on.[1–4] Inspired by the magic of nature, such as lotus leaves, petals and butterfly wings, the construction of a superhydrophobic surface requires two conditions: the roughness of the surface micro/nanostructures and a compound with a low surface tension.[5–7] Among all the materials, textiles, especially cotton fabric, which is inexpensive, renewable, flexible and easy to hybridize, was one of the most promising candidates for the construction of micro/nanostructures combined with low surface tension components for preparing the superhydrophobic products.[8,9]

There are several types of materials and methods to construct a micro/nano hierarchical structure on the surface of cotton fabric. Huang *et al.* successfully developed TiO_2 particles on the surface of cotton fabric similar to the structure of a petal's surface, with good mechanical properties, environmental stability, better self-cleaning performance and oil–water separation efficiency.[10] Shah *et al.* developed Al_2O_3 nanoparticles and a PDMS composite coating, and achieved an excellent superhydrophobic effect (WCA = 165°).[11] Zhu reported a simple method to prepare ZnO and a PDMS hybrid on the fabric, which showed excellent superhydrophobic properties, self-cleaning properties and UV resistance, as well as wear and wash resistance.[12] Wang *et al.* introduced two adjacent transition metals (Fe and Co) to be nanoparticles and *n*-octadecyl thiol to be the components of low surface tension to prepare a surface with superhydrophobicity (CA > 150°).[13] Also, nano-SiO_2 is the most widely reported and used, attributed to its low-cost, easy modification, and eco-friendly nature.[14–18]

However, the adhesion of rough nano silica particles on cotton fabric is not ideal, and it is easy for them to peel off, thus with the reported superhydrophobic materials it is still difficult to achieve the wear and scratch resistance. Therefore, finding materials and methods that could not only reduce the surface tension, but also improve the wear and scratch resistance is crucial.[14] Cao *et al.* reported that a nano-rough surface was formed by a silica aerogel, and then a superhydrophobic cotton fabric was prepared using a PDMS coating. The contact angle (CA) was greater than 160° and the rolling angle was less than 10°. It had good anti-fouling, self-cleaning, and high-efficiency

[a]*College of Biomass Science and Engineering, Sichuan University, Chengdu 610065, PR China. E-mail: dzl407@163.com; Tel: +86-28-85401296*

[b]*National Engineering Research Centre of Clean Technology in Leather Industry, Sichuan University, Chengdu 610065, PR China. E-mail: scuchx@163.com*

oil–water separation performances. The superhydrophobic material could endure 100 cycles of wear resistance (3.5 kPa) and five cycles of repeated mechanical washing.[19] Pan *et al.* prepared a PDMS-$CuSA_2$ superhydrophobic coating on cotton fabric using an *in situ* method with dip coating method with sodium hydroxide etching. The WCA of the prepared fabric could reach 158° and the coating had excellent chemical stability and UV resistance. The efficiency of oil–water separation was more than 90% and the fabric had good reusability. The as-prepared material can withstand 10 cycles (100 g) of mechanical abrasion.[20] However, these methods relied on the affinity between PDMS and the fabric itself, and the traditional high-temperature baking method was time-consuming and energy-consuming. In particular, the preparation of a superhydrophobic fabric coating with good wear resistance and high separation efficiency for oil/water mixture still has great challenges.[20]

Herein, a UV curable fluorine-free superhydrophobic coated, and wear-resistant cotton fabric was prepared by a simple method and applied in oil–water separation (Scheme 1). Firstly, sulfhydryl silica nanoparticles were prepared on the surface of the fabric *via* a Stöber reaction (SiO_2–SH@cotton). Then, the side chain hydroxyl terminated PDMS was reacted with isocyanate to form an isocyanate terminated prepolymer. The prepolymer terminated by HEMA (vinyl-terminated PDMS (PIH)) was sprayed onto the fabric surface, and then the superhydrophobic coating (SiO_2–S–PIH@cotton) was formed by UV curing. A series of characterization methods were used to demonstrate the structure of modified fabric. In particular, it was found that the as-prepared fabric had excellent wear resistance. Compared with that before spraying, the superhydrophobicity of the as-prepared fabric showed no obvious decrease after 300 cycles under 200 g of weight, and the wear resistance reached more than 100 cycles under circular friction of 500 g. This process was time-saving, energy-saving, environmentally friendly, had a low material cost and a strong performance stability. It is hoped that this fabric could be applied in the large-scale industrialization of oil–water separation.

2. Experimental section

2.1 Materials

Tetraethyl orthosilicate (TEOS), 3-mercaptopropyltriethoxysilane (MPTES), ethanol (EtOH) aqueous ammonia ($NH_3 \cdot H_2O$, 25 wt%), dibutyltin didodecylate (DBTDL, 90%) hydroxyethyl methacrylate (HEMA), 2-hydroxy-2-methylpropiophenone (Darocur 1173), isophorone diisocyanate (IPDI) and methyl alcohol were supplied by the Huaxia Chemical Industry Co., Ltd (Chengdu, China). Hydroxyl terminated organosilicon (PDMS, X-22-176B, $M_n = 2600$) was supplied by Shin-Etsu Chemical Co., Ltd (Japan). There was no further purification before use of any of the chemical reagents. Dichloromethane (DCM), *n*-hexane (NH), bromobenzene (BB), trichloromethane (TCM), petroleum ether (PE) and tetrahydrofuran (THF) were purchased from Tansoole. Cotton fabric (desized and scoured, woven, 106 g m^{-2}) was purchased from Dragon Clan (China) Co., Ltd., (Fujian, China). The pristine cotton fabric was pre-treated with deionized (DI) water with ultrasonic cleaning before use.

2.2 Sample preparation

The preparation of a sample was divided into two steps. Firstly, the silica particles were reacted on the cotton fabric *via* the Stöber reaction. The original fabric (5 g) was pre-wetted by immersing it in TM solution (100 ml, consisting of EtOH, TEOS and MPTES).[13] The weight ratio of EtOH, TEOS, and MPTES in solution was 6 : 3 : 1. Next, the pre-treated fabric was put into a sealed beaker filled with an ammonia atmosphere and reacted at 50 °C for 20 min. The fabric (named SiO_2–SH@cotton) was obtained after drying for 1 h at 80 °C.

In the second step (see Scheme 2), PIH (IPDI 0.01 mol, PDMS 0.005 mol, HEMA 0.01 mol) was synthesized first (PIH: $M_n = 3.66 \times 10^4$ g mol^{-1}, $M_w = 7.84 \times 10^4$ g mol^{-1}), and then the photo-initiator 1173 X was added. Next compounding solution was sprayed onto the surface of the SiO_2–SH@cotton. Subsequently, the sprayed fabric was placed under UV light (365 nm, 120 mW cm^{-2}) and allowed to cure for 5 min at a distance of

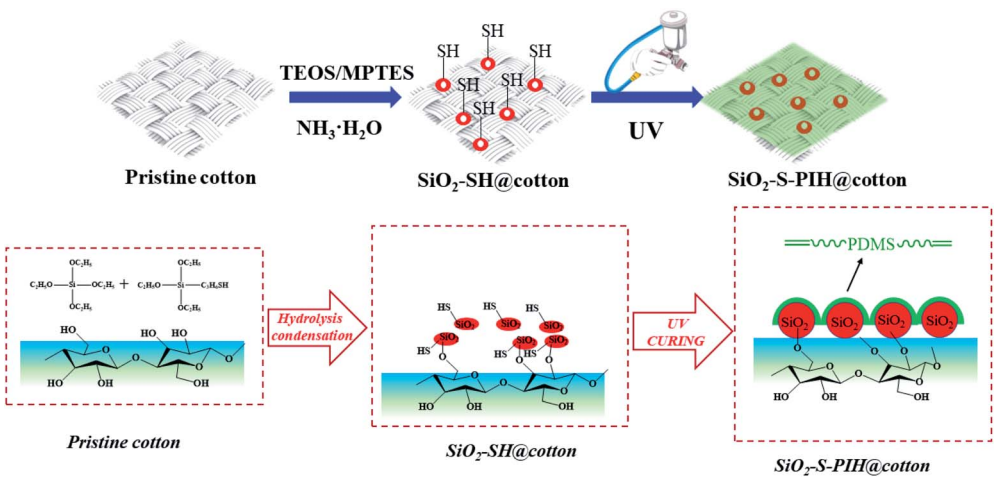

Scheme 1 Preparation of SiO_2–SH@cotton and SiO_2–S–PIH@cotton.

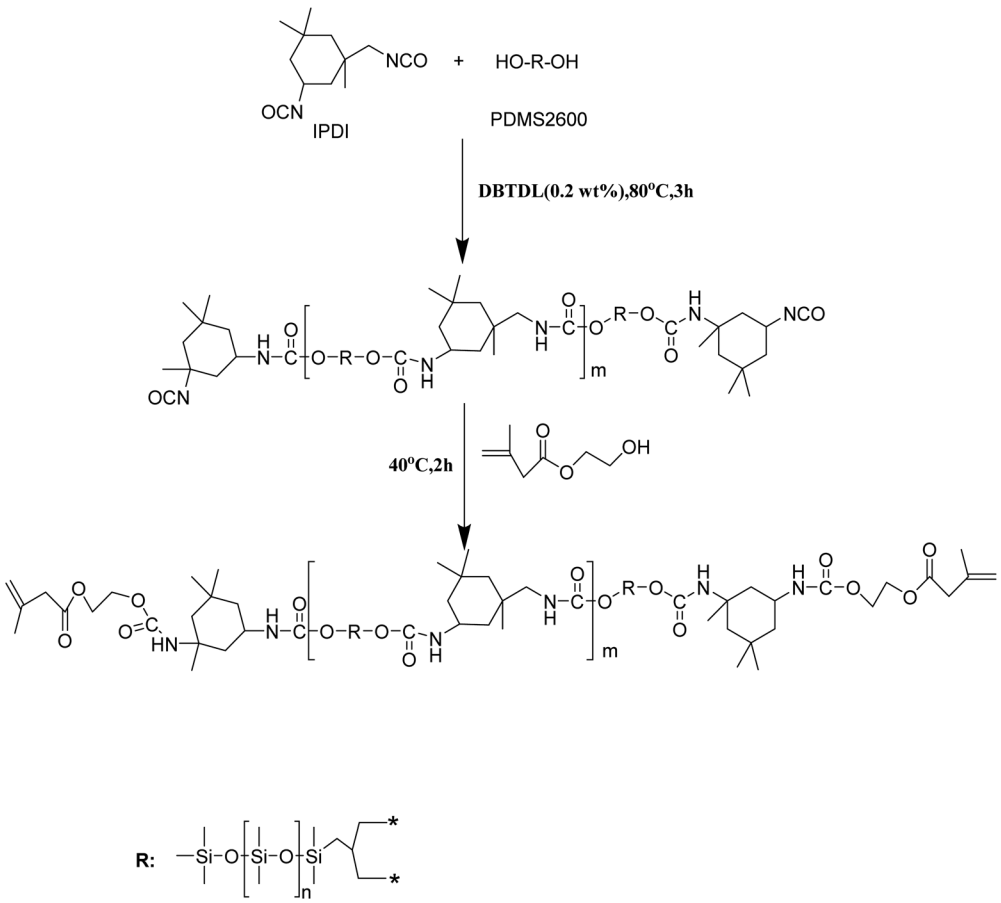

Scheme 2 Synthetic route for obtaining vinyl-terminated PDMS (PIH).

10 cm from the UV light. In this way, the superhydrophobic cotton fabric (SiO_2–S–PIH@cotton) was finally obtained.

2.3 Characterization

Fourier-transform infrared spectroscopy (FT-IR) and X-ray photoelectron spectroscopy (XPS) were performed with a Nicolet 560 FT-IR spectrometer (Nicolet, USA) in the range of 400–4000 cm^{-1} and XSAM800 instrument (Kratos Analytical, UK), respectively. X-ray diffraction (XRD) was conducted to research the crystallization of the samples using a D8 advance diffractometer (Bruker) in the range of 5°–60°. The thermodynamic stability of the cotton fabric was determined suing TGA and DTG (TA Instruments, USA) from 50° to 800 °C. The test conditions were as: heating rate: 20 °C min^{-1}, under N_2 and air atmosphere. Cotton samples were tested by thermogravimetry-IR (TG-IR) spectroscopy to determine the combustion products of the cotton samples with a STA 8000 TG-IR spectrometer (Perkin Elmer, USA). The limiting oxygen index (LOI) was measured by the vertical combustion method given in the GB/T5454-1997 standard. The size of the cotton sample was 150 mm (length) × 58 mm (width). The morphology of the cotton fibers before and after modification as well as the char residues after cone calorimetry testing (CCT) were characterized using scanning electron microscopy energy-dispersive X-ray spectroscopy SEM-EDX analysis with a JSM-7500F instrument (SEM, JSM-7500F, Jeol, Japan). The standard for the CCT combustion test method is the ISO 5660-1 standard, using a cone calorimeter (Fire Testing Technology, UK). The size was 100 mm (length) × 100 mm (width). The washing resistance of the cotton fabric before and after modification was determined using the AATCC 61-2006 standard. The tensile strength and elongation at break of the cotton fabrics were measured according to the GB/T3923-1997 standard test method. At least three measurements for each sample (25 cm × 5 cm) were recorded. The flexibility of the fabric samples was evaluated according to ASTM D1388-96 (2002) test method. The bending rigidity of the fabrics was measured using eqn (1):

$$G = M \times C^3 \quad (1)$$

where, G, M and C are the bending rigidity (mg cm), the cotton fabric weight (mg cm^{-2}) and the average bending length (cm), respectively. The WCAs in the air and the sliding angles (SA) were measured using the DSA25S contact angle measuring device (Krüss, Germany). Deionized water (*i.e.*, 5 μL for the static contact angle, 15 μL for the SA) was used as a testing liquid in this research.

The weight gain (WG) was calculated using the following eqn (2):

$$\mathrm{WG}(\%) = \frac{W_1 - W_0}{W_0} \times 100\% \quad (2)$$

where W_0 is the weight of the SiO_2–SH@cotton fabric and W_1 is the weight of SiO_2–S–PIH@cotton fabric.

2.4 Self-cleaning test and stability evaluation

The cotton fabric before and after modification was covered with the powder impurity coating, buried in the soil, and then taken out to compare the dirt on it after flushing with a small amount of water. Chemical stability was measured using the following experiment. The treated textile was soaked in various chemical solutions, such as acid (pH = 2, hydrochloric acid), alkali (pH = 11, sodium hydroxide), NaCl solution, DCM, NH, toluene, coffee and milk for 48 h. After the treatments were finished, the WCA tests were applied to assess the chemical durability of the treated fabrics. Furthermore, the anti-ultrasonic treatment capability was investigated by using a UV lamp to light the fabric, followed by determination of the WCAs of the surface every 20 min.

2.5 Oil and water separation experiment

Oil/water separation is the primary function of the fabric. In this study, light oil (NH) and heavy oil (DCM) were prepared for use

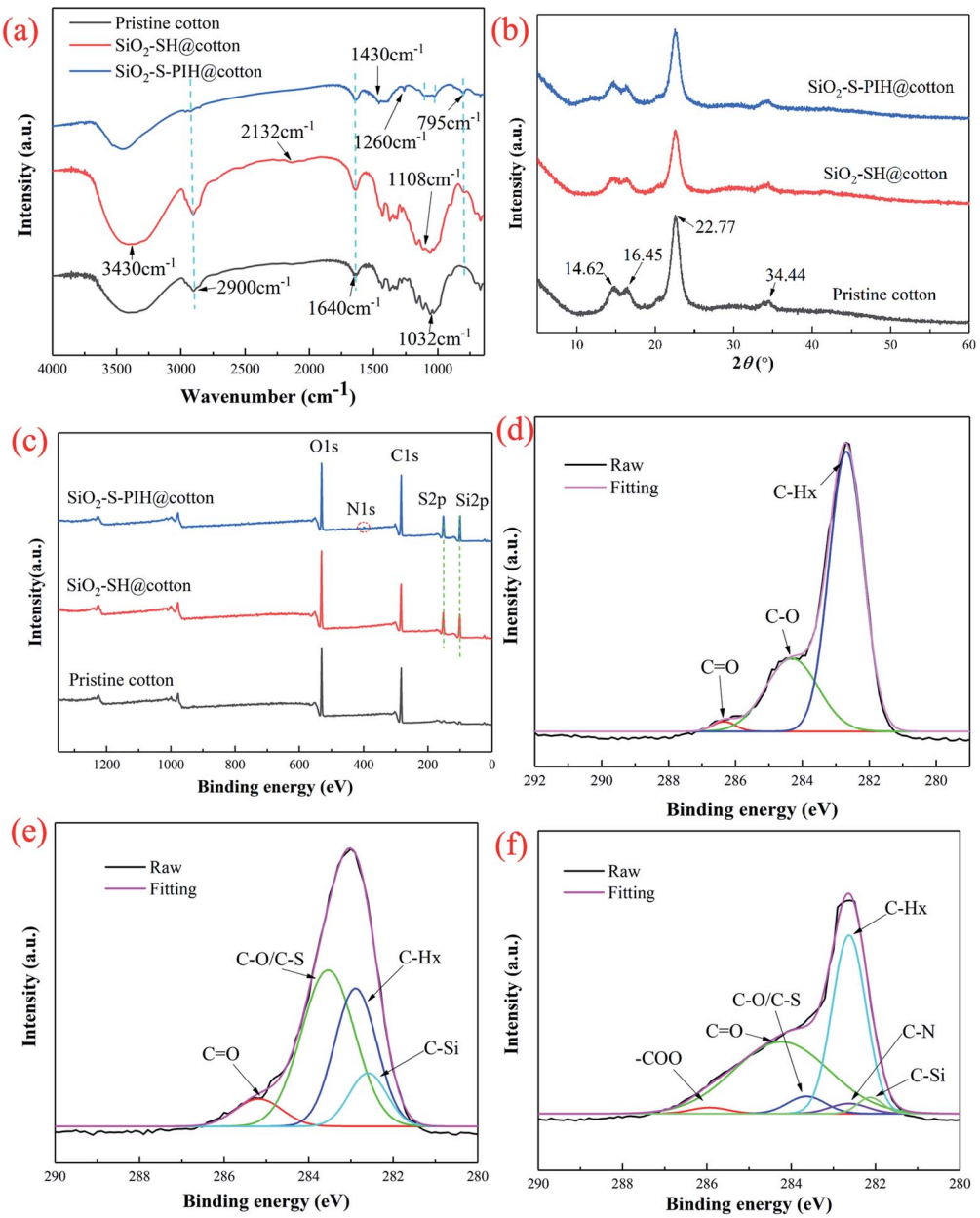

Fig. 1 (a) The FT-IR spectra of pristine cotton fabric, SiO_2–SH@cotton and SiO_2–S–PIH@cotton. (b) The XRD of pristine cotton, SiO_2–SH@cotton and SiO_2–S–PIH@cotton. (c) The XPS spectra of the pristine cotton fabric, SiO_2–SH@cotton and SiO_2–S–PIH@cotton. The high-resolution XPS spectra of the C 1s region of (d) pristine cotton fabric, (e) SiO_2–SH@cotton and (f) SiO_2–S–PIH@cotton.

as two oil models to test the separation efficiency. Moreover, other heavy or light oils were also applied to assess the generalizability of the oil/water separation material. As shown later, this device was applied to oil/water separation tests. A mixture of 100 ml of red oil and 100 ml of blue water was put into the funnel container above the separation device.[21] Theoretically, the red oil passes through the filter into the beaker below but the blue water cannot penetrate the fabric and remains in the upper container. Additionally, the separation test was repeated for 30 cycles to study the repeatability of the use of the functional fabric. Eqn (3) was used to calculate the fabric separation efficiency rate:[22]

$$E_S = (m_1/m_2) \times 100\% \quad (3)$$

where m_1 and m_2 are the masses of solutions after and before the test, ordinally. Moreover, NH and DCM were considered to represent different densities of oil, respectively.

3. Results and discussion

3.1 Characterization

FT-IR, XRD and XPS were used to characterize the composition of the pristine cotton, the SiO_2–SH@cotton and the SiO_2–S–PIH@cotton to confirm whether the modification process was successful. The results of this are shown in Fig. 1. Firstly, the broad absorption peaks at 3430 cm^{-1}, 2900 cm^{-1} and 1640 cm^{-1} corresponded to the stretching vibrations of –OH, the stretching vibrations of $-CH_2$ and the bending vibrations of –OH, respectively, and these were the characteristic peaks of cellulose.[23] The bands at 1108 cm^{-1} and 795 cm^{-1} were assigned to the Si–O–Si stretching peaks. The peak at 2132 cm^{-1} was due to the stretching vibration peak of –SH which only appeared with the SiO_2–SH@cotton, which proved that SiO_2–SH@cotton had been fabricated successfully.[24,25] Meanwhile, a new peak appeared at 1430 cm^{-1} which was attributed to the stretching vibration of S–C. This showed that the double bond of HEMA reacted with the sulfhydryl radical after the UV curing reaction. The peak at 1260 cm^{-1} only appeared when modification of the cotton surface was attributed to Si–C, which also confirmed that PDMS and MPTES were successfully coated on to the cotton fabric.[26]

Then the crystal structures of the four types of cotton fibers were determined by XRD, and the results are clearly shown in Fig. 1b. The peak values of the pristine cotton fiber were found at the $2\theta = 14.62°$, 16.45°, 22.75° and 34.44° positions, which corresponded to the crystal planes of cellulose-I (1−10), (110), (200) and (004), respectively.[27,28] The crystal structure of the modified cotton fiber was consistent with that of the pristine cotton fabric and the intensity of the peak had decreased slightly. These structures indicated that a series of chemical modifications had not changed the crystal structure of the cotton fiber.

Finally, the chemical components on the surface of the cotton fabrics were further determined using XPS, as shown in Fig. 1c–f. As shown in Fig. 1c, the pristine cotton fabric included C 1s (283.2 eV) and O 1s (531.3 eV) peaks, whereas two new peaks, S 2p (162.5 eV) and Si 2p (101.8 eV), appeared after the modification of the silica particles (SiO_2–SH@cotton) and N 1s (398.6 eV) appeared on the cotton fabric after spraying with PIH.

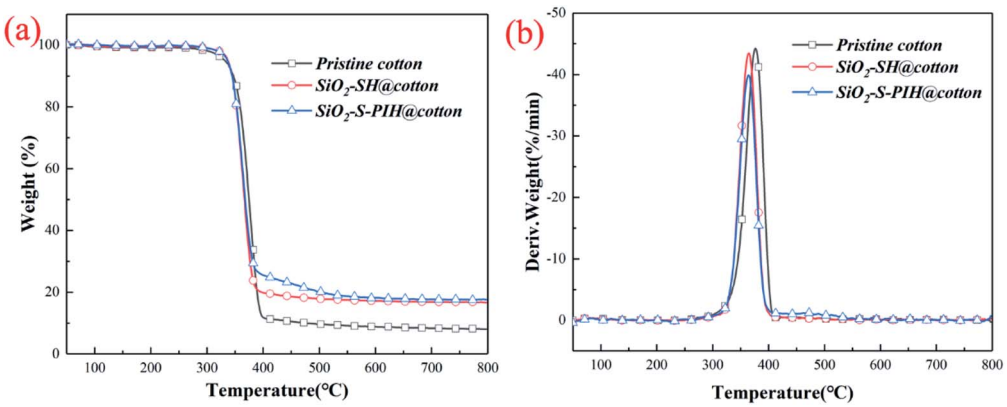

Fig. 2 The TGA (a) and DTG (b) curves of pristine cotton, SiO_2–SH@cotton and SiO_2–S–PIH@cotton under a N_2 atmosphere.

Table 1 Characteristic parameters of TGA and DTG curves for cotton under a N_2 atmosphere[a]

Sample	$T_{5\%}$ (°C)	T_{max} (°C)	R_{max} (wt% per min)	Residue at 800 °C (wt%)
Pristine cotton	330	377	44.2	8
SiO_2–SH@cotton	334	362	43.2	17.5
SiO_2–S–PIH@cotton	338	361	39.5	18.8

[a] $T_{5\%}$ is the temperature at which the mass loss is 5 wt%, T_{max} is the temperature at which the mass loss rate is maximum, R_{max} is the the maximum mass loss rate.

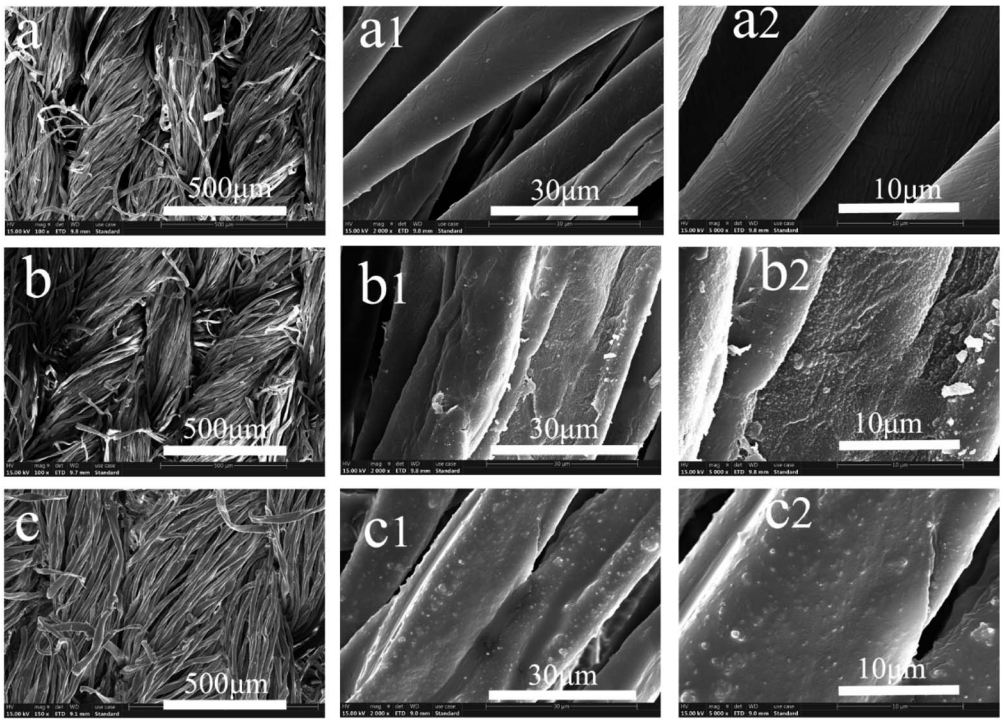

Fig. 3 SEM images of pristine cotton (a), SiO_2–SH@cotton (b) and SiO_2–S–PIH@cotton (c) at 100, 2000, and 5000 SE, respectively.

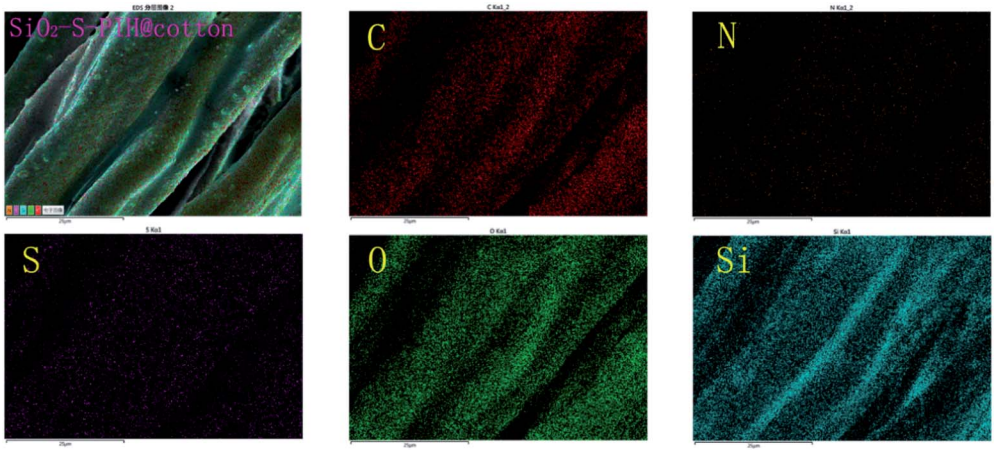

Fig. 4 EDX elemental mapping images of carbon, nitrogen, sulfur, silicon, and oxygen of SiO_2–S–PIH@cotton at 2000 SE.

These XPS results showed that silica particles and PIH polymers were successfully grafted onto the fabric.[29,30] Based on the XPS analysis of C 1s, it was found that C–Hx (C–C, C–H, C=C, 283.15 eV), C–O (284.42 eV), C=O (286.3 eV) were included in pristine cotton. Compared with pristine cotton, it could be seen from Fig. 1e that the groups of two new peaks (C–O/C–S, 284.22 eV and C–Si, 282.81 eV) also appeared, which proved that the silica particles with the sulfhydryl group had been modified successfully. At the same time, it can be seen from Fig. 1f that two peaks were added (–COO, 286.68 eV and C–N, 282.92 eV), which indicated that the reaction of thiol with a double bond was successful, and that of isocyanate and polyol was successful.[31,32]

3.2 Thermogravimetric analysis (TGA)

In order to compare the change of thermal stability of the cotton fabric before and after modification, TGA and DTG were used, and the results are shown in Fig. 2. Various related parameters are also listed in Table 1. It can be seen from Table 1 that the $T_{5\%}$ of the modified cotton fabric had obviously increased and the thermal stabilities of the as-prepared cottons were improved. The improvement of the thermodynamic properties of the modified fabric was beneficial for applications of the fabric.

3.3 Morphology analysis

As mentioned, previously, superhydrophobicity requires two conditions: a rough nano surface and a low surface tension

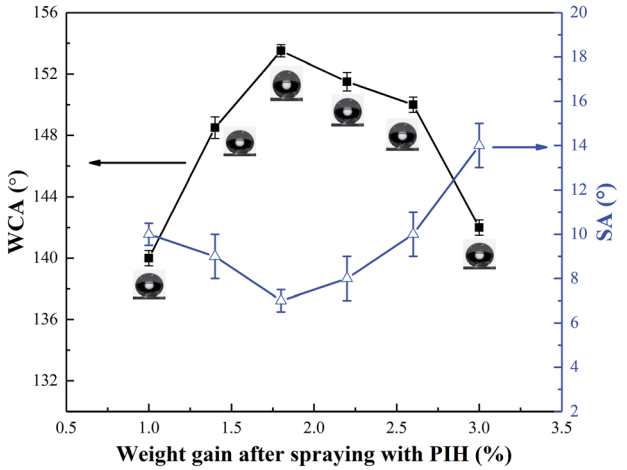

Fig. 5 The WCAs and SAs of cottons with different weight gains after spraying with PIH.

surface. The material studied here was examined by SEM, and the clear images can be seen in Fig. 3. It can be seen from Fig. 3 that the surface of the pristine cotton was smooth. After the TEOS and MPTES modification, dense small particles grew over the surface of the cotton and covered the whole fibre surface (Fig. 3b).

It should be noted that the silica particles were formed on the fiber surface by a sol–gel method. This is consistent with a phenomenon reported previously in the literature. From Fig. 3c, it can be seen that the surface of the silica particles was coated with a very thin coating, which should be the PIH that was sprayed on, before the light curing reaction. This structure should be helpful for superhydrophobic capacity and durability.

The EDX mapping was further used to investigate the element distribution of SiO_2–S–PIH@cotton fabric. It was clearly seen that the elements of C, O, N, S, and Si were dispersed uniformly (Fig. 4). In summary, the previous results confirmed that the SiO_2 nanoparticles had been formed and that PIH was distributed uniformly on the surface.

3.4 Weight gain after spraying with PIH

In order to study the effect of weight gain after spraying with PIH on superhydrophobicity, the change of WCA between 1%–3% weight gain, was measured and the results are shown in the Fig. 5. With the increase of the quantity of PIH, the WCA increased first and then decreased. When the weight of the spray coating was 1.8%, the maximum WCA was 153° and the maximum SA was 7°. The reason for this is that the rough surface and the low surface tension coating need to achieve a balance, too little PIH, is insufficient to support the low surface tension, whereas with too much PIH, it was easy to completely cover the silica particles, and the roughness was reduced. It can be seen from Fig. 5, that the trend of the change of SAs was consistent with that of the WCAs. Therefore, a weight gain of 1.8% after spraying with PIH was selected as the optimum in this research.

3.5 Flexibility of superhydrophobic cotton fabric

As a fabric still in the implementation process, the mechanical strength and softness are very important parameters. In order to study the mechanical properties and softness of the modified fabric, the stress–strain curve and bending rigidity were determined, and the results are shown in Fig. 6. It can be seen from Fig. 6a that the pristine cotton fabric has a good mechanical property. After the first step of modification (SiO_2–SH@cotton), the rigidity was enhanced and the elongation decreased slightly. This should be due to the formation of rigid silica particles on the fabric surface, and the cellulose structure was slightly damaged in the ammonia atmosphere. After spraying PIH (WG = 1.8%), the breaking strength of the fabric continued to increase, but the elongation at break decreased. This was due to the formation of a film on the surface of the fabric after PIH curing, which increased the strength. But it may also be due to the binding of the yarn, which limited the yarn movement and lead to the decrease of elongation at break. Bending rigidity of the treated cotton fabrics with different weight gains after spraying with different amounts of PIHs is shown in Fig. 6b. The rigidity of the SiO_2–

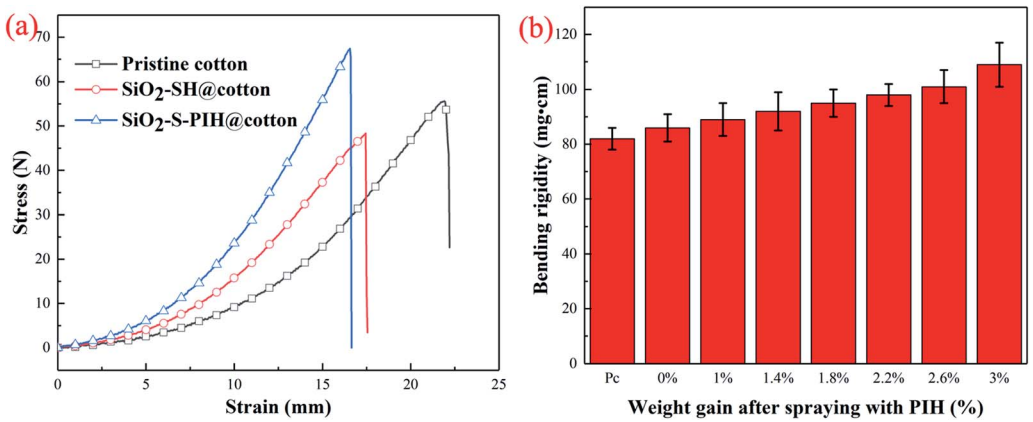

Fig. 6 (a) Strain–stress curve of the cotton fabric sample. (b) Bending rigidity and weight gain of the treated cotton fabrics after spraying different amounts of PIH (Pc: pristine cotton).

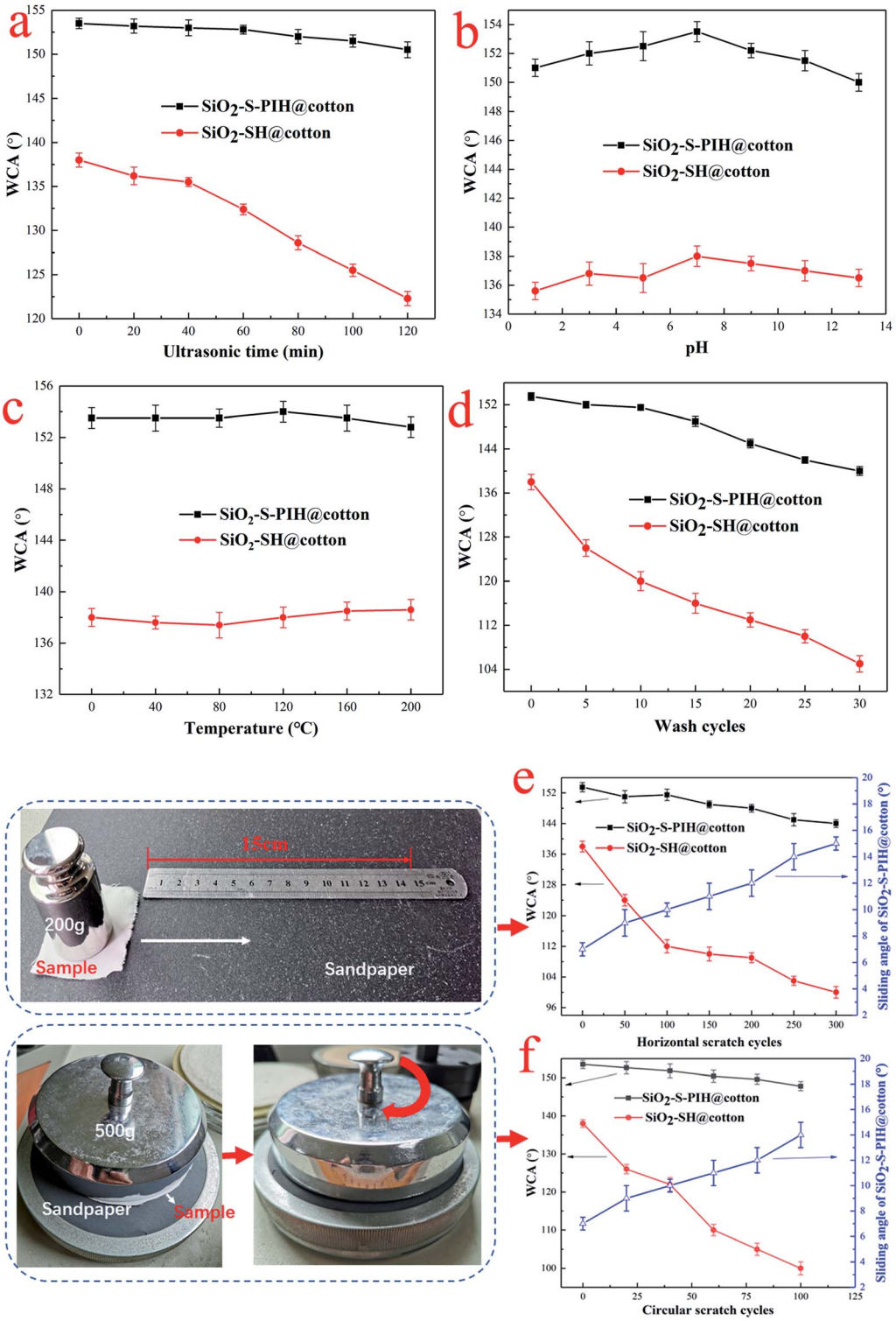

Fig. 7 The influence of (a) ultrasonic treatment, (b) solutions with different pH values, (c) placed under different temperatures for 6 h, and (d) wash cycles. Effect of (e) horizontal scratch cycles, and (f) circular scratches, on WCAs and SAs of SiO_2–SH@cotton and SiO_2–S–PIH@cotton.

SH@cotton fabric was higher than that of the pristine cotton fabric. With the increase of the amount of PIH sprayed, the rigidity of the fabric increased. This result was consistent with the stress–strain curve. Although the mechanical strength of the modified cotton fabric showed some changes, its flexibility was still very good, which is very important for the subsequent applications of the cotton.

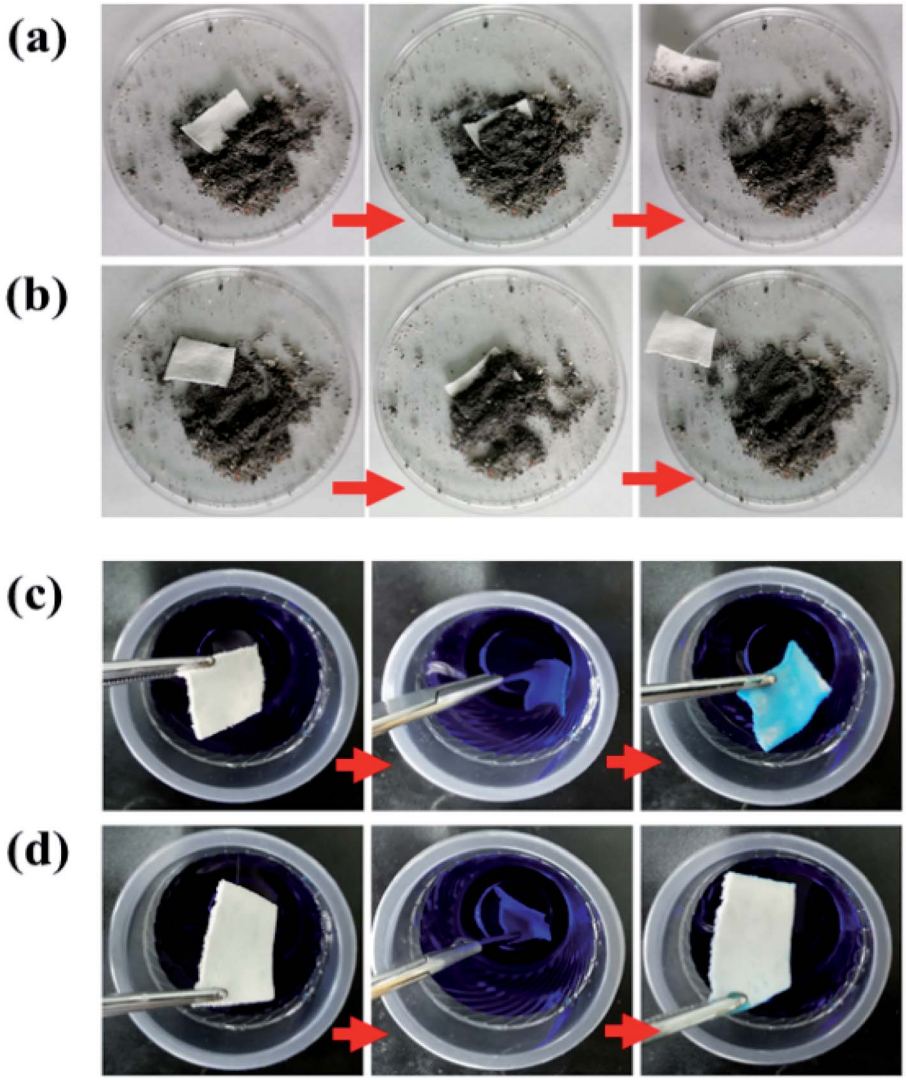

Fig. 8 Self-cleaning ability of (a) pristine cotton textile and (b) SiO_2–S–PIH@cotton with powder contaminants. Self-cleaning ability of (c) pristine cotton textile and (d) SiO_2–S–PIH@cotton in polluted solutions.

3.6 Durability of superhydrophobic cotton fabric

The durability and stability of modified fabrics is very important when considering their practical applications. As shown in Fig. 7a, when the fabric sample was placed in the ultrasonic processor, it could be observed that the WCA of the SiO_2–S–PIH@cotton decreased slightly with the extension of the ultrasonic wave, and it still remained above 150° after 120 min, but the decrease of SiO_2–SH@cotton was faster, which may be caused by insufficient adhesion of the silica particles on the surface and partial shedding. Fig. 7b shows the change of the WCA of the fabric surface after the fabric was immersed in solutions with different pH for 48 h. Both samples were not sensitive to the change of pH value, and the WCA decreased slightly in acidic and alkaline conditions. Fig. 7c shows the curve of the influence of temperature change on the WCA. The samples were baked for 6 h at each temperature. It can be seen from the figure that the two samples were not sensitive to temperature change. Even if they were baked at 200 °C for 6 h, their WCAs were remained stable. This showed that the modified fabric had excellent high temperature resistance.

Fastness of fabrics when washed in water is an important index to measure the superhydrophobicity of fabric. In Fig. 7d, the materials were washed according to a standard washing method, and the change of WCA was tested. It can be seen from Fig. 7d that the WCA of SiO_2–S–PIH@cotton decreased slightly with the increase of washing time, and it remained above 138° after 30 cycles of washing. The WCA of SiO_2–SH@cotton decreased rapidly with the increase of washing time, which may be due to the insufficient adhesion of the nanoparticles.

Finally, the main idea of this research was to improve the wear resistance of superhydrophobic fabrics, so two methods were used to evaluate the wear resistance of the modified fabrics. The first method was the horizontal scratch method, results are shown in Fig. 7e, which involves friction back and

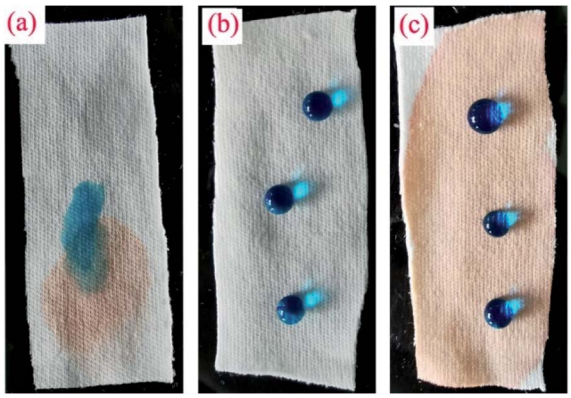

Fig. 9 (a) Photograph of water (dyed with MB) and dichloromethane (dyed with OR) on a pristine textile. (b) Photograph of water droplets on SiO_2–S–PIH@cotton. (c) Photograph of water droplets and *n*-hexane on SiO_2–S–PIH@cotton.

forth on the surface of 15 cm sandpaper (2000 mesh), and then the WCA was measured after the friction. The results showed that the wear resistance of the SiO_2–S–PIH@cotton was very good, and it was still above 144° after 300 cycles, whereas the WCA of the SiO_2–SH@cotton decreased greatly after friction. The first reason for this was that the nanoparticles easily fell off the surface under friction if there was no protective layer, and the superhydrophobic effect became worse. In the circular scratch method (Fig. 7f), the test results were similar to those of the first method. In addition, from Fig. 7, it can be seen that the trend of the change of the SAs was consistent with that of the WCAs. Therefore, the SiO_2–S–PIH@cotton had excellent friction resistance, and the abrasion resistance of the superhydrophobic fabric could be solved by a spraying and UV curing method.

3.7 Self-cleaning

The results of the self-cleaning ability testing of the fabrics is shown in Fig. 8. When the two types of cotton fabrics were inserted into fine powder contaminants at the same time, and then taken out, and were then flushed with a small amount of water, it was found that SiO_2–S–PIH@cotton was free from dust and had a self-cleaning function similar to the lotus leaf surface, whereas the unmodified cotton fabric was still covered with dust (Fig. 8a and b). The results of another test are shown in Fig. 8c and d. For this test two fabrics were simultaneously inserted into a bluish colored aqueous solution, where pristine cotton immediately absorbed the blue liquid whereas the SiO_2–S–PIH@cotton remained clean. The sample SiO_2–S–PIH@cotton could also float on the water surface without external force. These results all indicate that SiO_2–S–PIH@cotton is superhydrophobic with self-cleaning ability, which is conducive to its further application in the field of outdoor decorations and household appliances.

3.8 Oil–water separation

As shown in Fig. 9, the pristine cotton fabric could absorb both water and oil. The SiO_2–S–PIH@cotton was completely lipophilic, and after absorbing oil and then dropping water solution on it, there was still good hydrophobicity. Based on this characteristic, SiO_2–S–PIH@cotton could be used in the field of oil–water separation. The fabric was used to absorb a light oil (NH, dyed with OR) and heavy oil (DCM, dyed with OR), and the results are shown in Fig. 10. This small piece of cotton fabric could easily absorb the light oil floating on the water and the heavy oil sank into the water. These results proved that the SiO_2–S–PIH@cotton had a great potential in the field of oil–water separation.

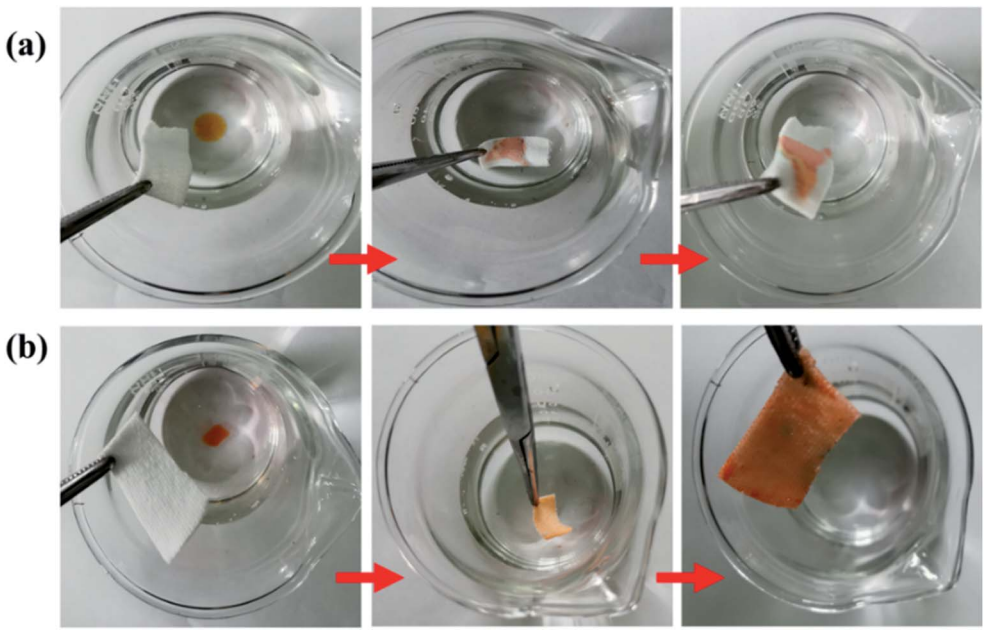

Fig. 10 Absorption processes of (a) light oil (*n*-hexane, dyed with OR) and (b) heavy oil (dichloromethane, dyed with OR) from water using SiO_2–S–PIH@cotton.

Fig. 11 Photographs of the oil–water separation process with SiO_2–S–PIH@cotton.

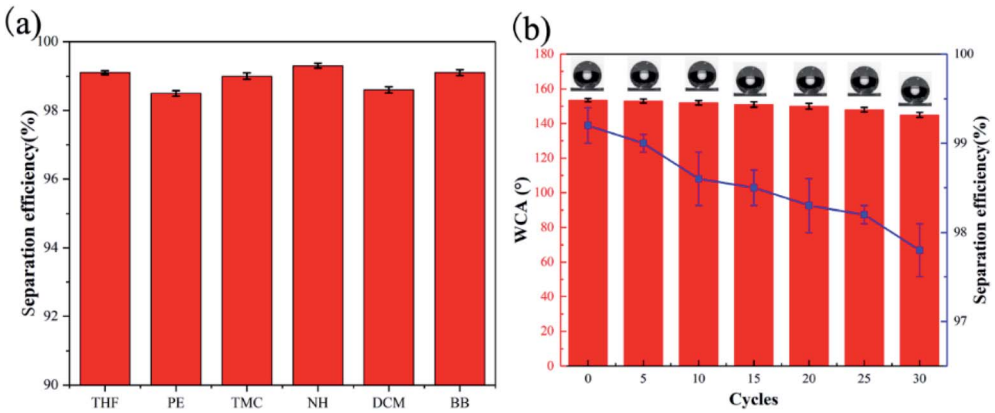

Fig. 12 (a) The separation efficiency of SiO_2–S–PIH@cotton for various oil–water mixtures. (b) The variation of separation efficiency and WCA of SiO_2–S–PIH@cotton *versus* the number of separation cycles.

Therefore, representative oil–water separation was used to verify the oil–water separation efficiency. Fig. 11 shows the oil–water separation device and oil–water separation program. Heavy oil (DCM) was chosen as an oil model to test the separation performance. The results showed that when the oil–water mixture was poured into the separation device, the oil easily leaked through the fabric into the conical flask, and the water was tightly blocked above, so it achieved the purpose of oil–water separation. The experiment proved that SiO_2–S–PIH@cotton has excellent oil–water separation efficiency, and the separation efficiency reaches more than 99.1%.

In order to verify the applicability of SiO_2–S–PIH@cotton, the oil–water mixture was prepared with different types of oil and was then treated with the same oil–water separation method. The results are shown in Fig. 12a and b, which proved that there was a good separation effect (more than 98.5%) for the six simulated oils. In addition, the durability of the fabric was verified by repeated filtration and separation cycles. The results showed that after 30 cycles of repeated use, the filtration efficiency was still above 97.8%, and the WCA of SiO_2–S–PIH@cotton was still greater than 145°. Thus, the SiO_2–S–PIH@cotton had an efficient oil–water separation ability and reusability.

4. Conclusion

A durable, superhydrophobic, self-cleaning cotton fabric based on UV curing was prepared by a simple method and used in the field of oil–water separation. A series of characterization methods were used to demonstrate the material's structure. When the weight gain after PIH spraying was 1.8%, the fabric reaches an optimal state with a WCA of 153° and a SA of 7°. The superhydrophobic fabric shows excellent chemical and environmental stability under the optimal conditions. When used in an oil–water separation test, the highest separation efficiency could reach 99.1%. In particular, it was found that the as-prepared fabric has excellent wear resistance compared with that before spraying with PIH. In both the horizontal wear test and the circular wear test, the superhydrophobic durability of SiO_2–S–PIH@cotton was much better than that of SiO_2–SH@cotton. This indicated that the surface sprayed polymers have two functions: (i) providing low surface tension, and (ii) protecting the rough surface formed by silica particles. This process was time-saving, energy-saving, environmentally friendly, had a low material cost and strong performance stability. It is hoped that this method can be used in the large-scale industrialization of oil–water separation.

Conflicts of interest

There are no conflicts to declare.

Acknowledgements

This work was funded by the National Natural Science Foundation of China (No. 51773129 and 51903167), the Support Plan of Science and Technology Department of Sichuan Province, China (2019YFG0257 and 2020YFG0071), the Miaozi Project in Science and Technology Innovation Program of Sichuan Province (20-YCG045). We also appreciate the help of Mi Zhou and Sha Deng for their assistance with the experimental testing.

References

1 W. Cao, Y. Liu, M. Ma and J. Zhu, *Colloids Surf., A*, 2017, **529**, 18–25.
2 E. Cho, C. Chang-Jian, H. Chen, K. Chuang, J. Zheng, Y. Hsiao, K. Lee and J. Huang, *Chem. Eng. J.*, 2017, **314**, 347–357.
3 Q. Liu, J. Huang, J. Zhang, Y. Hong, Y. Wan, Q. Wang, M. Gong, Z. Wu and C. F. Guo, *ACS Appl. Mater. Interfaces*, 2018, **10**, 2026–2032.
4 L. Xu, Y. Guo, L. Liu, G. Bai, J. Shi, L. Zhang, X. Chang, R. Zhang, J. Zhang and J. Yu, *Prog. Org. Coat.*, 2020, **146**, 105727.
5 S. Dey, S. Chatterjee, B. P. Singh, S. Bhattacharjee, T. K. Rout, D. K. Sengupta and L. Besra, *Surf. Coat. Technol.*, 2018, **341**, 24–30.
6 G. Caputo, B. Cortese, C. Nobile, M. Salerno, R. Cingolani, G. Gigli, P. D. Cozzoli and A. Athanassiou, *Adv. Funct. Mater.*, 2009, **19**, 1149–1157.
7 J. Ou, J. Ma, F. Wang, W. Li, X. Fang, S. Lei and A. Amirfazli, *Prog. Org. Coat.*, 2020, **147**, 105777.
8 L. Cai, L. Dai, Y. Yuan, A. Liu and L. Zhanxiong, *Appl. Surf. Sci.*, 2016, **371**, 453–467.
9 S. Roy, L. Zhai, J. W. Kim, H. C. Kim and J. Kim, *Prog. Org. Coat.*, 2020, **140**, 105500.
10 J. Y. Huang, S. H. Li, M. Z. Ge, L. N. Wang, T. L. Xing, G. Q. Chen, X. F. Liu, S. S. Al-Deyab, K. Q. Zhang, T. Chen and Y. K. Lai, *J. Mater. Chem. A*, 2015, **3**, 2825–2832.
11 S. Maryam Shah, U. Zulfiqar, S. Z. Hussain, I. Ahmad, Habib-ur-Rehman, I. Hussain and T. Subhani, *Mater. Lett.*, 2017, **203**, 17–20.
12 T. Zhu, S. Li, J. Huang, M. Mihailiasa and Y. Lai, *Mater. Des.*, 2017, **134**, 342–351.
13 B. Wang, Y. Zhang, W. Liang, G. Wang, Z. Guo and W. Liu, *J. Mater. Chem. A*, 2014, **2**, 7845–7852.
14 J. Chen, Y. Zhou, C. Zhou, X. Wen, S. Xu, J. Cheng and P. Pi, *Chem. Eng. J.*, 2019, **370**, 1218–1227.
15 S. Li, J. Huang, Z. Chen, G. Chen and Y. Lai, *J. Mater. Chem. A*, 2017, **5**, 31–55.
16 M. Yang, W. Liu, C. Jiang, C. Liu, S. He, Y. Xie and Z. Wang, *Ind. Eng. Chem. Res.*, 2019, **58**, 187–194.
17 H. Zhou, H. Wang, H. Niu, A. Gestos, X. Wang and T. Lin, *Adv. Mater.*, 2012, **24**, 2409–2412.
18 J. Li, L. Yan, X. Tang, H. Feng, D. Hu and F. Zha, *Adv. Mater. Interfaces*, 2016, **3**, 1500770.
19 C. Cao, M. Ge, J. Huang, S. Li, S. Deng, S. Zhang, Z. Chen, K. Zhang, S. S. Al-Deyab and Y. Lai, *J. Mater. Chem. A*, 2016, **4**, 12179–12187.
20 G. Pan, X. Xiao and Z. Ye, *Surf. Coat. Technol.*, 2019, **360**, 318–328.
21 L. Jin, Y. Wang, T. Xue, J. Xie, Y. Xu, Y. Yao and X. Li, *Langmuir*, 2019, **35**, 14473–14480.
22 Y. Yang, Z. Guo, W. Huang, S. Zhang, J. Huang, H. Yang, Y. Zhou, W. Xu and S. Gu, *Appl. Surf. Sci.*, 2020, **503**, 144079.
23 M. Yang, W. Liu, C. Jiang, S. He, Y. Xie and Z. Wang, *Carbohydr. Polym.*, 2018, **197**, 75–82.
24 S. Y. L. B. Yan, *J. Bionic Eng.*, 2017, **14**, 497–505.
25 J. Lin, X. Wu, C. Zheng, P. Zhang, B. Huang, N. Guo and L. Jin, *Appl. Surf. Sci.*, 2014, **303**, 67–75.
26 U. Zulfiqar and A. Habib-ur-Rehman, *Colloids Surf., A*, 2018, **539**, 391–398.
27 W. Kwak, M. H. Oh and M. Gong, *Carbohydr. Polym.*, 2015, **115**, 317–324.
28 C. Tian, C. Wang, X. Ren and L. Hong, *J. Appl. Polym. Sci.*, 2019, **136**, 47199.
29 K. Hou, Y. Zeng, C. Zhou, J. Chen, X. Wen, S. Xu, J. Cheng and P. Pi, *Chem. Eng. J.*, 2018, **332**, 150–159.
30 C. Xue, X. Guo, M. Zhang, J. Ma and S. Jia, *J. Mater. Chem. A*, 2015, **3**, 21797–21804.
31 F. Chen, Y. Zhu, W. Li, J. Yang, P. Fan, Z. Fei, M. Zhong, L. Chang and T. Kuang, *Appl. Surf. Sci.*, 2019, **464**, 273–279.
32 H. Wang, C. Zhang, J. Wang, X. Feng and C. He, *ACS Sustainable Chem. Eng.*, 2016, **4**, 3803–3811.